High-throughput microfluidic blood testing to phenotype genetically linked platelet disorders: an aid to diagnosis

REGULAR ARTICLE

blood advances

High-throughput microfluidic blood testing to phenotype genetically linked platelet disorders: an aid to diagnosis

Delia I. Fernandez,[1,2] Isabella Provenzale,[1,3] Matthias Canault,[4] Salome Fels,[5] Antonia Lenz,[5] Felicia Andresen,[5] Anne Krümpel,[6] Arnaud Dupuis,[7] Johan W. M. Heemskerk,[1,8,*] Doris Boeckelmann,[5,*] and Barbara Zieger[5,*]

[1]Department of Biochemistry, Cardiovascular Research Institute Maastricht (CARIM), Maastricht University, Maastricht, The Netherlands; [2]Platelet Proteomics Group, Center for Research in Molecular Medicine and Chronic Diseases, Universidad de Santiago de Compostela, Santiago de Compostela, Spain; [3]Institute for Cardiovascular and Metabolic Research, University of Reading, Reading, United Kingdom; [4]Institut National de la Santé et de la Recherche Médicale, UMR_INRA 1260, Faculté de Medecine, Aix Marseille Université, Marseille, France; [5]Department of Pediatrics and Adolescent Medicine, Division of Pediatric Hematology and Oncology, Medical Center, University of Freiburg, Freiburg, Germany; [6]Practice for Pediatric and Youth Medicine, Wettringen, Germany; [7]Université de Strasbourg, Etablissement Français du Sang Grand Est, UMR_S 1255, Fédération de Médecine Translationnelle de Strasbourg, Strasbourg, France; and [8]Synapse Research Institute, Maastricht, The Netherlands

Key Points

- Linking the genetic background of patients with a platelet function disorder to bleeding diathesis is challenging.
- Microfluidic multiparameter testing of thrombus formation can aid in the identification of a platelet disorder.

Linking the genetic background of patients with bleeding diathesis and altered platelet function remains challenging. We aimed to assess how a multiparameter microspot-based measurement of thrombus formation under flow can help identify patients with a platelet bleeding disorder. For this purpose, we studied 16 patients presenting with bleeding and/or albinism and suspected platelet dysfunction and 15 relatives. Genotyping of patients revealed a novel biallelic pathogenic variant in *RASGRP2* (splice site c.240-1G>A), abrogating CalDAG-GEFI expression, compound heterozygosity (c.537del, c.571A>T) in *P2RY12*, affecting $P2Y_{12}$ signaling, and heterozygous variants of unknown significance in the *P2RY12* and *HPS3* genes. Other patients were confirmed to have Hermansky-Pudlak syndrome type 1 or 3. In 5 patients, no genetic variant was found. Platelet functions were assessed via routine laboratory measurements. Blood samples from all subjects and day controls were screened for blood cell counts and microfluidic outcomes on 6 surfaces (48 parameters) in comparison with those of a reference cohort of healthy subjects. Differential analysis of the microfluidic data showed that the key parameters of thrombus formation were compromised in the 16 index patients. Principal component analysis revealed separate clusters of patients vs heterozygous family members and control subjects. Clusters were further segregated based on inclusion of hematologic values and laboratory measurements. Subject ranking indicated an overall impairment in thrombus formation in patients carrying a (likely) pathogenic variant of the genes but not in asymptomatic relatives. Taken together, our results indicate the advantages of testing for multiparametric thrombus formation in this patient population.

Introduction

Platelet bleeding disorders are highly heterogeneous, with clinical manifestations ranging from a prolonged bleeding time, incidental mucocutaneous bleeding, easy bruising, and menorrhagia to life-threatening

Submitted 27 January 2023; accepted 30 May 2023; prepublished online on *Blood Advances* First Edition 30 June 2023; final version published online 13 October 2023. https://doi.org/10.1182/bloodadvances.2023009860.

*J.W.M.H., D.B., and B.Z. contributed equally to this study.

Indirect data are available on request from the corresponding author, Barbara Zieger (barbara.zieger@uniklinik-freiburg.de).

The full-text version of this article contains a data supplement.

bleeding episodes.[1,2] Despite extensive efforts, the underlying genetic cause of a bleeding disorder in many of the cases remains elusive.[3,4] Routine platelet function tests, developed by consensus parties, provide an improved diagnostic workflow for revealing platelet disorders but are still imperfect in patient identification.[5-7]

The common platforms for the analysis of platelet function are light transmission aggregometry (LTA) and flow cytometry, often in combination with von Willebrand factor (VWF) measurements and standard coagulation times.[7,8] In particular, flow cytometry has been shown to be useful for confirming storage pool deficiency (SPD) of platelets, displaying an impairment in δ-granule secretion (marker CD63) and/or α-granule secretion (marker CD62P).[9,10] As an additive tool, sequencing analysis of a defined set of platelet-expressed genes (panel sequencing) has become useful for identifying inherited platelet defects; however, the power of this tool remains limited.[11,12]

Large microfluidic testing for proxy hemostasis has mainly been performed with whole blood from 32 patients with von Willebrand disease, showing the importance of VWF in shear-dependent platelet aggregation and thrombus formation.[13] Recently, we established a multiparameter microfluidic assay based on 6 defined microspots for detailed platelet phenotyping from 97 healthy subjects, which provided 48 outcome parameters of platelet activation under flow leading to thrombus formation.[14] This study revealed that particular collagen-dependent thrombus characteristics are associated with common genetic variants of *GP6* (encoding glycoprotein VI, GPVI) and *FCER1G* (encoding the Fc receptor γ-chain). In another study, microfluidic testing of blood from patients with combined immunodeficiency and bleeding indicated compromised collagen-dependent formation of thrombi linked to pathogenic variants of the *STIM1* and *ORAI1* genes.[15] Although proof-of-principle evidence is available that microfluidic measurement of thrombus formation can detect platelet defects,[16,17] this testing has not yet been performed in larger patient cohorts.

Here, we describe microfluidic testing of blood from 11 families with a (likely) congenital platelet defect. These included patients with a new CalDAG-GEFI defect (biallelic novel *RASGRP2* variant) and a $P2Y_{12}$ receptor defect (compound heterozygous variants in *P2RY12*). In addition, we investigated families with variants of uncertain significance (VUS) in *P2RY12* (monoallelic) or *HPS3* (compound heterozygous) as well as families with pathogenic variants in *HSP1* and *HSP3* genes. By combining the characteristics of thrombus formation with routine platelet function tests, we evaluated the potential of microspot-based microfluidics as an additional tool for detecting a platelet bleeding disorder.

Methods

A detailed description of the methods and patients is available in the supplemental Methods.

Patients and control subjects

This study was conducted in accordance with the Declaration of Helsinki and approved by the ethics committee of Albert-Ludwigs-University Freiburg (584/17, 28 August 2018). All patients were recruited from the outpatient clinic of the Department of Pediatrics and Adolescent Medicine at the University Medical Center, Freiburg. Patients with a previously assessed platelet bleeding disorder who were subjected to genetic screening along with consenting family members were reinvited for microfluidic testing and blood cell evaluation in September 2019. All included patients, non-affected family members, and healthy control subjects gave written informed consent. High-content microfluidic blood testing was performed at the Medical Center, Freiburg. An extensive phenotypic description of the index patients and family members, for convenience all labeled as "Pat," with genetic analysis is presented in the supplemental Materials; supplemental Table 1. None of the subjects had used antiplatelet medications for at least 14 days. Reference data were obtained from day-control subjects (indicated as CCF) and a previously published cohort of 97 healthy subjects (94 fully genotyped; indicated as CCB).[14]

Blood preparation and platelet aggregation

Blood samples were collected in 3.2% trisodium citrate vacuette tubes and used for all assays. Common hematologic parameters were obtained using an automated cell counter (Sysmex KX-21 N, Norderstedt, Germany). For index patients and available family members, platelet aggregometry (APACT4) with normalized platelet-rich plasma was performed1[18]; the agonist panel consisted of 2 μg/mL collagen (Takeda, Linz, Austria), 4 μM adenosine 5′-diphosphate (ADP) (Sigma-Aldrich, St Louis, MO), 8 μM epinephrine (Sanofi-Aventis, Frankfurt, Germany), and 1.2 mg/mL ristocetin (American Biochemical and Pharmaceutical, Frankfurt, Germany). Where indicated, 5 μM TRAP6 (Hart Biologicals, Hartlepool, United Kingdom) and 0.5 mg/mL arachidonic acid (MöLab, Langenfeld, Germany) were added to the panel.

Molecular genetic analysis

For indicated patients, genomic DNA was extracted from EDTA-anticoagulated blood using a QIAamp DNA Blood Mini Kit (Qiagen, Hilden, Germany). Next-generation sequencing was performed using a 95-gene panel (custom-designed Nextera Rapid Enrichment Kit, Illumina), as previously described.[19] Sequence Pilot (JSI Medical Systems) and Alamut Visual Plus (Sophia Genetics) packages were used for bioinformatic analysis. The pathogenicity of the suspected variants was deduced in silico using the combined annotation-dependent depletion, PolyPhen2, and SIFT packages. The variants were classified based on the guidelines of the American College of Medical Genetics.[20] Confirmation of potentially pathogenic variants and segregation analyses were performed using direct sequencing.

For patients with a biallelic *RASGRP2* canonical splice-site variant, complementary DNA (cDNA) sequencing was performed. Total RNA was isolated from washed human platelets using the Trizol reagent (Thermo Fisher, Waltham, MA). Single-stranded cDNA was generated using SuperScript III reverse transcriptase (Thermo Fisher). The primers used for amplification and sequencing were forward CTTCGATGACTCCGGGAAGG and reverse GATCATGAGCTGCACCCACT, which cover the *RASGRP2* coding region from exon 2 to exon 7. For family 2, with a suspected ADP receptor defect, direct sequencing was performed of the candidate gene *P2RY12*. Genetic analysis of other patients and family members was reported in earlier work (supplemental Table 1).

Microspot-induced multiparameter thrombus formation under flow

Microfluidic measurements of thrombus formation to assess platelet adhesion, activation, and aggregation under flow were

performed using microspot-coated flow chambers, through which recalcified, PPACK-anticoagulated blood was perfused.[14] Immediately before perfusion, citrated blood samples were anticoagulated with 40 μM PPACK and recalcified with 3.75 mM $MgCl_2$ and 7.5 mM $CaCl_2$. This procedure allows for the testing of blood under physiological divalent cation concentrations, resulting in optimized platelet adhesion and aggregation under flow.[16]

Blood perfusion over the microspots was for 3.5 minutes at a wall-shear rate of 1000/s. The adhered platelets forming thrombi were triple-stained with fluorescein isothiocyanate-labeled antifibrinogen monoclonal antibody (mAb), Alexa Fluor (AF)568 annexin A5, and AF647 anti-CD62P mAb (supplemental Methods). Microscopic images were acquired using an EVOS-FL microscope (Life Technologies, Bleiswijk, The Netherlands) equipped with 3 fluorescent light-emitting diodes combined with dichroic cubes (Cy5, for red fluorescent protein, and for green fluorescent protein), an Olympus UPLSAPO 60× oil-immersion objective, and a sensitive 1360 × 1024 pixel charged-coupled device camera.

The microspots in the flow chambers were labeled from most to least active, as indicated in supplemental Table 2: *M1*, collagen type 1; *M2*, GFOGER-GPO + VWF-binding peptide (VWF-BP); *M3*, collagen type 3; *M4*, rhodocytin + VWF-BP; *M5*, laminin + VWF-BP; *M6*, human fibrinogen + VWF-BP. The labeling order was determined via clustering analysis of the parameter values.

Brightfield and fluorescence images of each microspot were obtained before and after staining, respectively.[14] Duplicate flow runs were performed when possible. Semiautomated scripts using a manual threshold setting were used for standardized image analysis in the open-access program Fiji (supplemental Methods). Scoring of images was performed by observers blinded to the condition in comparison with reference images across microspots (supplemental Figure 1A). Outcome parameters were defined as follows: *P1*, platelet deposition (%SAC); *P2*, platelet multilayers (%SAC); *P3*, thrombus multilayer score (scale, 0-3); *P4*, thrombus contraction score (scale, 0-3); *P5*, thrombus morphological score (scale, 0-5); *P6*, integrin αIIbβ3 activation (fluorescein isothiocyanate antifibrinogen mAb); *P7*, P-selectin expression (AF647 anti-CD62P mAb); and *P8*, phosphatidylserine exposure (AF568–annexin A5). The number of microspots *M1-6* and parameters *P1-8* were uniform for all included subjects, including the reference cohort.

Results

Patient cohort and genetic variants

To evaluate how the multiparameter measurement of thrombus formation under flow can identify patients with a platelet bleeding disorder, we included 16 patients from 11 families, 15 unaffected family members (either heterozygous carriers or wild-type), and 5 CCFs (Table 1). Patients were selected based on earlier evidence of platelet dysfunction and the presence of (possibly) pathogenic genetic variants linked to dysfunction. The assay was performed in September 2019 in the outpatient clinic of the Department of Pediatrics and Adolescent Medicine at the University Medical Center of Freiburg, along with conventional measurements of hematologic parameters, LTA, and flow cytometry. The full genetic and diagnostic information of the index patients and family members is given in the supplemental Methods. For convenience, all members were labeled as Pat01-31 (index patients indicated by *). A comprehensive description is given for genetics of patients, including Pat01-15 and Pat22, who have not been fully described.

CalDAG-GEFI deficiency

The index patient Pat01* (family 1) presented to the outpatient clinic at the age of 3 years with a history of bleeding (International Society of Thrombosis and Haemostasis Bleeding Assessment Tool [ISTH-BAT] score of 7).[21] Platelet aggregation in response to ADP, collagen, epinephrine, and TRAP6 was severely impaired, in contrast to ristocetin-induced agglutination (Figure 1A). Flow cytometry showed normal platelet expression of the platelet receptor αIIbβ3 (Figure 1B) but impaired ADP-induced fibrinogen binding (Figure 1C). Panel sequencing revealed a novel homozygous pathogenic variant in the *RASGRP2* gene, located at the acceptor splice site of intron 4 (NM_153819.1:c.240-1G>A; Figure 1D). The variant (rs1490853368) was absent from the Human Gene Mutation Database. Genotyping confirmed a familial *RASGRP2* variant (Figure 1E), and a founder effect was suspected based on the relationship between the 6 generations. cDNA sequencing of platelet-derived RNA helped confirm a skip of exon 5 (Figure 1F). Immunoblotting helped confirm the absence of CalDAG-GEFI protein in the patient's platelets (Figure 1G). Of the 3 heterozygous family members (Pat02-04, low ISTH bleeding scores of 2, 2, and 0), only the father's platelets showed slightly impaired platelet aggregation, whereas fibrinogen binding was normal (supplemental Datafile 1).

$P2Y_{12}$ receptor defects

Index patients Pat05* and Pat06* (family 2) were twins with severe bleeding after trauma and surgery (Table 1). Platelet aggregometry showed major impairments in the response to ADP.[22] Flow cytometry indicated an essentially abolished fibrinogen binding in response to ADP in both patients (supplemental Methods), suggesting a $P2Y_{12}$ receptor deficiency.[23] Direct sequencing of *P2RY12* (NM_022788.4) and family genotyping revealed the compound heterozygosity of 2 novel (likely) pathogenic variants (c.537del and c.571A>T) in both children. The variants led to a premature stop codon and an amino acid change (supplemental Table 1). The Asn191Tyr change is located in the transmembrane domain of the ADP ligand-binding pocket, according to crystal structure analysis.[24] Pat07 (mother) was heterozygous for c.571A>T and did not exhibit bleeding symptoms. Pat08* (family 3) had a history of mild bleeding after tonsillectomy. Panel sequencing revealed a heterozygous variant of *P2RY12* (c.853T>C; p.Trp285Arg), which was predicted to be deleterious (supplemental Methods). Platelet fibrinogen binding after stimulation with ADP was reduced. The variant segregated with this platelet phenotype in 2 affected children (not included). Mild bleeding symptoms have earlier been associated with the presence of a heterozygous *P2RY12* variant.[25,26] We classified c.853T>C as a VUS because of this first description.

Unresolved storage pool deficiencies

Family 4, consisting of a mother (Pat09*) and 2 affected sons (Pat10* and Pat11*), presented with a moderate-to-severe bleeding phenotype combined with a platelet storage pool defect (reduced expression of CD62P and mildly of CD63; Table 1). Platelet aggregometry was impaired in response to collagen, ADP, ristocetin, and epinephrine in all 3 probands (supplemental

Table 1. General characteristics of included patients and control subjects

Subject	Family	Diagnosis and genetics	Age	M/F	Phenotype	PLT (10^9/L)	RBC (10^9/L)	Mean LTA	FC-SPD mean
CCF	N/A	CCFs (n = 5)	25-48	2/3	Healthy controls	277 ± 42	4.2 ± 0.2	0.0	0.0
CCB	N/A	CCBs (n = 97)	25-79	38/59	Healthy, blood type O	268 ± 58	4.6 ± 0.4	n.d.	n.d.
Pat01*	Fam1	CalDAG-GEFI deficiency (AR)	4	M	Severe bleeding	263	4.0	−2.0	0.0
Pat02	Fam1	Carrier *RASGRP2* pathogenic variant	49	M	Healthy family member	145	4.7	−1.3	0.0
Pat03	Fam1	Carrier *RASGRP2* pathogenic variant	44	F	Healthy family member	190	4.0	0.0	0.0
Pat04	Fam1	Carrier *RASGRP2* pathogenic variant	10	F	Healthy family member	288	4.5	0.0	n.d.
Pat05*	Fam2	P2Y12 receptor defect (AR, CH)	9	M	Severe bleeding	280	4.5	−1.3	0.0
Pat06*	Fam2	P2Y12 receptor defect (AR, CH)	9	M	Severe bleeding	298	4.3	−1.3	0.0
Pat07	Fam2	Carrier *P2RY12* likely pathogenic variant	42	F	Healthy family member	217	4.0	n.d.	n.d.
Pat08*	Fam3	P2Y12 receptor defect? variant of uncertain significance	33	M	Mild bleeding	204	4.4	−1.3	−0.3
Pat09*	Fam4	SPD + TCP	41	F	Moderate bleeding	94	3.6	−1.3	−1.5
Pat10*	Fam4	SPD + TCP; VWD-1 pathogenic variant	20	M	Moderate bleeding	65	3.8	−1.3	−1.5
Pat11*	Fam4	SPD + TCP; VWD-1 pathogenic variant	18	M	Moderate bleeding	86	3.9	−1.3	−1.5
Pat12	Fam4	No SPD, VWD-1 pathogenic variant	46	M	Healthy family member	163	4.4	0.0	0.0
Pat13*	Fam5	δ-SPD, no variant identified	18	M	Moderate bleeding	198	4.8	−1.7	−1.0
Pat14*	Fam5	δ-SPD, no variant identified	60	F	Moderate bleeding	212	3.9	−0.7	−0.5
Pat15	Fam5	Unaffected family member	62	M	Healthy family member	201	4.2	0.0	0.0
Pat16*	Fam6	HPS-3 (AR), δ-SPD	17	M	Oculocutaneous albinism	213	4.5	−1.7	−0.7
Pat17	Fam6	Carrier *HPS3* pathogenic variant	47	F	Healthy family member	209	4.0	−1.0	0.0
Pat18	Fam6	Carrier *HPS3* pathogenic variant	25	F	Healthy family member	185	4.0	n.d.	n.d.
Pat19*	Fam7	δ-SPD, HPS3 (CH) VUS	7	F	Ocular albinism	192	4.1	−1.3	−1.0
Pat20	Fam7	Carrier variant in *HPS3*	47	M	Healthy family member	221	4.5	−1.0	n.d.
Pat21*	Fam8	HPS-1 (AR, CH), δ-SPD	16	M	Oculocutaneous albinism	228	4.4	−0.7	−1.0
Pat22	Fam8	Carrier *HPS1* pathogenic variant	7	F	Healthy family member	172	3.9	0	−1.0
Pat23	Fam8	Carrier *HPS1* pathogenic variant	50	M	Healthy family member	203	4.7	0	n.d.
Pat24*	Fam9	HPS-1 (AR, CH), δ-SPD	11	M	Oculocutaneous albinism	329	4.0	−0.3	−1.5
Pat25	Fam9	Carrier HPS1 pathogenic variant	49	F	Healthy family member	261	4.5	n.d.	n.d.
Pat26	Fam9	Wild type in family genotyping	19	M	Healthy family member	183	4.9	0.0	n.d.
Pat27	Fam9	Carrier *HPS1* pathogenic variant	53	M	Healthy family member	210	4.7	0.0	n.d.
Pat28*	Fam10	HPS-1 (AR, CH), δ-SPD	9	M	Oculocutaneous albinism	354	4.3	−1.3	−1.5
Pat29*	Fam10	HPS-1 (AR, CH), δ-SPD	5	M	Oculocutaneous albinism	309	3.9	−1.7	−1.5
Pat30	Fam10	Carrier *HPS1* pathogenic variant	33	F	Healthy family member	227	4.1	n.d.	n.d.
Pat31*	Fam11	HPS-1 (AR, CH), δ-SPD	30	M	Oculocutaneous albinism	181	4.8	−1.7	−1.0

Indicated are controls (day control cohort CCF; reference control cohort CCB), index patients (*), and relatives, arranged per family (Fam). Further indicated are sex, global phenotype, platelet (10^9/L), and red blood cell (10^{12}/L) counts. In addition, mean defects in platelet aggregation (scored for ADP, collagen, epinephrine, and ristocetin) or in secretion marker exposure by flow cytometry, estimating SPD (FC-SPD: thrombin-induced P-selectin and CD63 expression).

Red color intensity indicates degree of reduction. Codes per measurement: 0, within the normal range; −1, below the normal range; and −2, below 50% of the normal range.

For an extended description of the patients, genetic analyses, and references, see supplemental Materials and supplemental Table 1.

AR, autosomal recessive; AD, autosomal dominant; CH, compound heterozygous; Fam, family; F, female; FC-SPD, flow cytometry-SPD; M, male; n.d., not determined; N/A, not applicable; PLT, platelet; RBC, red blood cell.

Datafile). The father, Pat12, was not affected. The molecular genetic analysis did not identify a possible cause for SPD or moderate thrombocytopenia (TCP). However, this revealed a heterozygous pathogenic variant (c.7987C>T, p.Arg2663Cys) in the *VWF* gene in the unaffected father and 2 sons but not in the mother. The plasma VWF parameters in all subjects were normal (supplemental Methods). In family 5, the index patient (Pat13*) and his mother (Pat14*) had mild-to-moderate bleeding problems and a platelet δ-granule secretion defect, whereas the father (Pat15) was not affected. The panel sequencing did not reveal any pathogenic or likely pathogenic variants.

Hermansky-Pudlak syndromes 1 and 3

We investigated 5 patients with HPS type 1 (oculocutaneous albinism and platelet δ–SPD, which were genetically confirmed) and their family members (families 8-11). The various pathogenic variants have been previously published by our group (supplemental Datafile; supplemental Methods). In all the index patients, platelet aggregation was impaired after stimulation with several agonists. Five clinically healthy family members had heterozygous genotype for a single variant, and 1 family member (Pat26) had wild-type genotype for segregating variants (Table 1).

In addition, members of 2 other families (families 6 and 7) with δ-SPD and variants in the *HPS3* gene (Table 1) were included. The index patient (Pat16*, of family 6 suffered from oculocutaneous albinism and platelet δ–SPD) was diagnosed with HPS type 3 (NM_032383.5:c.2771del; loss-of-function p.Asn924Ilefs*4).[27] Both unaffected family members Pat17 and Pat18 had heterozygous genotype for this variant. In family 7, Pat19* with δ-SPD (determined via flow cytometry) carried 2 novel compound heterozygous *HPS3* missense VUS (c.65C>G and c.1193G>A; supplemental Datafile). A specialized ophthalmological examination showed atypical albinism.[19] The father (Pat20) had heterozygous genotype for c.65C>G.

Impairments in whole blood thrombus formation in patients and family members

Based on whole blood thrombus formation data from the CCB of 97 healthy subjects,[14] we applied the multiparameter test for the phenotyping of blood samples from 31 patients with family members (Pats 01-31), which is 1 of the first cohorts of this size, with a known or expected platelet function disorder and bleeding phenotype. For comparison, we obtained blood samples from 5-day- CCFs.

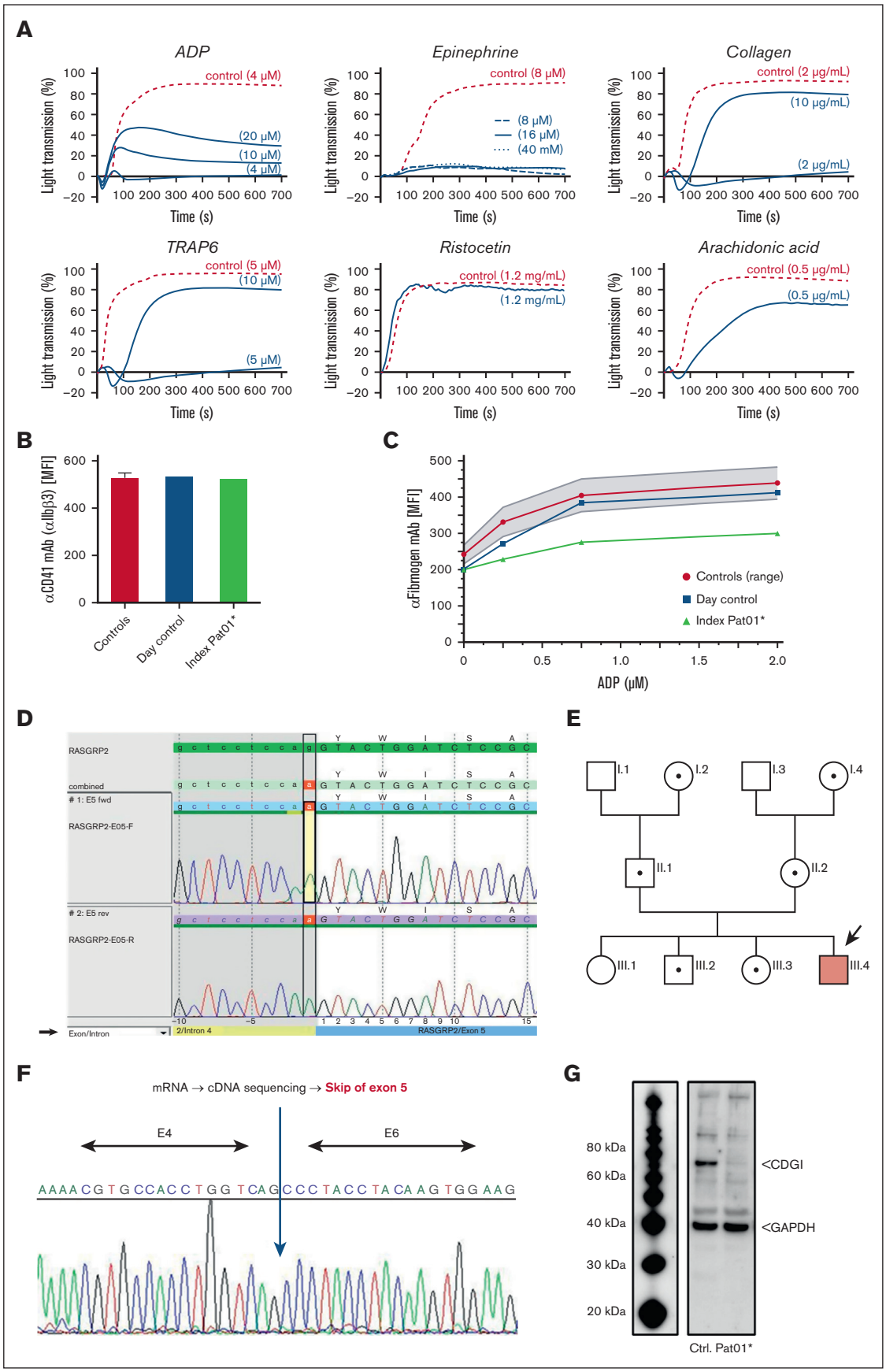

Figure 1.

For the assay, anticoagulated, recalcified blood samples from all subjects were perfused at a high wall-shear rate (1000/s) over 6 microspots (*M1-6*) and composed of collagen 1 (*M1*), collagen-like peptide GFOGERGPO + VWF-BP (*M2*), collagen 3 (*M3*), rhodocytin + VWF-BP (*M4*), laminin + VWF (*M5*), and fibrinogen + VWF-BP (*M6*) (supplemental Table 2). Brightfield and fluorescence images of the aggregated platelets under flow (thrombi) were used to obtain parameters of adhesion (*P1*), aggregation (*P2*), thrombus type (*P3-5*), and platelet activation (fibrinogen binding, P-selectin expression indicative of α-granule secretion, and phosphatidylserine exposure; *P6-8*). Accordingly, this analysis resulted in 6 × 8 = 48 thrombus parameters per blood sample.

In agreement with earlier findings,[14] perfusion of blood from CCFs over collagen 1 (*M1*) resulted in the formation of large, multilayered thrombi containing fibrinogen-binding platelets and collagen 3 (*M3*) in smaller-sized thrombi (Figure 2, top panels). In *M1*, the platelets formed contracted thrombi, as noticed previously.[16] This is in agreement with the finding that thrombus contraction under flow can occur in the absence of clotting.[28]

Regarding the other microspots, platelet adhesion and thrombus formation were higher on the GPVI-stimulating surface *M2* than on the other surfaces from *M4* to *M6* (supplemental Figure 2). Perfusion of the blood from index patients Pat01* (*RASGRP2* defect) and Pat10* (SPD with TCP) over *M1* and *M3* resulted in an essentially abolished thrombus formation (Figure 2). Less severe defects with smaller-sized thrombi were observed in the blood from Pat06* (*P2RY12* defect), Pat13* (δ-SPD), Pat19* (*HPS3* variants, δ-SPD), and Pat29* (HPS-1, δ-SPD).

Following our standard analysis, the thrombus values from the total cohort of patients and controls were univariate, scaled from 0 to 10 per parameter (*P1-8*) across all 6 microspots (*M1-6*) for an integrative comparison. Unsupervised hierarchical cluster analysis of the scaled data set resulted in the ordering of microspots from most to least active, that is, from *M1* to *M6* (supplemental Figure 3). The accordingly ordered heatmap showed overall differences in the thrombus parameters per microspot and displayed substantial heterogeneity between the individual blood samples (supplemental Figure 4A). We, then, calculated the changes in scaled values per patient relative to the in-study controls (filtered for changes outside the mean ± standard deviation of 2 controls). The constructed subtraction heatmap provided an overview of the deviant *MP* parameters for per subject Pat01-31 (supplemental Figure 4B). Overall, the largest negative effect sizes (green) were observed for microspots *M2* (GFOGERGPO + VWF-BP), *M3* (collagen 3), and *M5* (laminin + VWF). However, positive effect sizes (red) were observed for *M4* (rhodocytin + VWF-BP). The subtraction heatmap also illustrated the similarity of scaled parameter values between the CCFs and CCBs.

We reasoned that a nonfiltered display of the scaled parameters provided a more detailed insight into the small differences in thrombus formation between the patients. The cumulative changes in parameter values (vs those in CCFs) showed consistently reduced values for microspots *M1*, *M2*, *M3*, and *M5* for most index patients and smaller changes for the unaffected family members (Figure 3). The strongest negative changes were observed in Pat01* (*RASGRP2* defect), Pat05*, Pat06* (*P2RY12* defects), Pat08* (*P2RY12,* VUS), and the carrier Pat07 (Figure 3A-B). Low cumulative values on *M1-5* were also present for the affected Pats 09, 10, and 11* (genetically unsolved SPD and TCP) but not for the unaffected relative Pat12 (Figure 3C). For the families with SPD (HSP-1 or HSP-3), most of the index patients, but not the carrier family members, had low values on *M2*, *M3*, and *M5* (Figure 3D-J). Hence, this subtraction analysis suggests a separation of thrombus parameters between many index patients and unaffected family members.

To assess the cohesion of the scaled data set, we generated a Spearman correlation matrix by comparing all parameters within and across the microspots (supplemental Figure 5A). This matrix showed within each microspot *M1-5* relatively strong correlations between *P1* and *P8*, whereas for *M6*, the brightfield parameters betwen *P1* and *P5* were segregated from the fluorescence parameters between *P6* and *P8*. This discrepancy was also apparent in the matrix of *P* values (supplemental Figure 5B). When comparing the microspots pairwise, the highest cohesion of parameters was seen between *M1* and *M3*, that is, all platelet GPVI–stimulating surfaces (supplemental Figure 5A). Furthermore, across microspots, parameters related to platelet aggregation (*P2*, platelet multilayer; *P3*, thrombus multilayer score; *P4*, thrombus contraction score; *P5*, thrombus morphological score; and *P6*, integrin αIIbβ3 activation) correlated well with $R > 0.40$. This pointed to a subject-dependent factor in the progress of platelet aggregation, independent of the microspot type.

Integration of thrombus formation and hematologic parameters

In addition, we evaluated the interaction between blood cell count and thrombus formation parameters. Therefore, we combined the scaled 48 *MP* values with the simultaneously measured whole blood parameters (white and red blood cells and platelet count) using subtraction analysis vs the means of CCFs. The resulting clustered heatmap showed 2 main groups: index patients and most of the unaffected family members (Figure 4A).

Figure 1. Platelet characterization and molecular genetic analysis of Pat01* using a novel *RASGRP2* variant. (A) Aggregation of platelet-rich plasma (light transmission %) from Pat01* (blue curves) and healthy control (dotted red curve), induced by ADP (4-20 μM), epinephrine (8-40 μM), collagen H (2-10 μg/mL), TRAP6 (5-10 μM), or arachidonic acid (0.5 mg/mL). Platelet agglutination was induced using ristocetin (1.2 mg/mL). (B) Flow cytometric analysis of diluted platelet-rich plasma, showing normal expression of αIIbβ3 (CD41). (C) Flow cytometry indicating impaired ADP-induced fibrinogen binding to Pat1* platelets, compared with those of CCFs (20 measurements from 6 controls; mean ± standard deviation). (D) Verification of a homozygous *RASGRP2* canonical splice site variant by direct sequencing. (E) Pedigree after segregation analysis (brown symbol indicates affected Pat III.4; dotted symbol indicates heterozygous carrier). (F) Direct sequencing of platelet-derived cDNA showing skip of exon 5. (G) Absence of CalDAG-GEFI protein (CDGI) in patient platelets compared with that in a control subject via western blotting. GAPDH, glyceraldehyde-3-phosphate dehydrogenase.

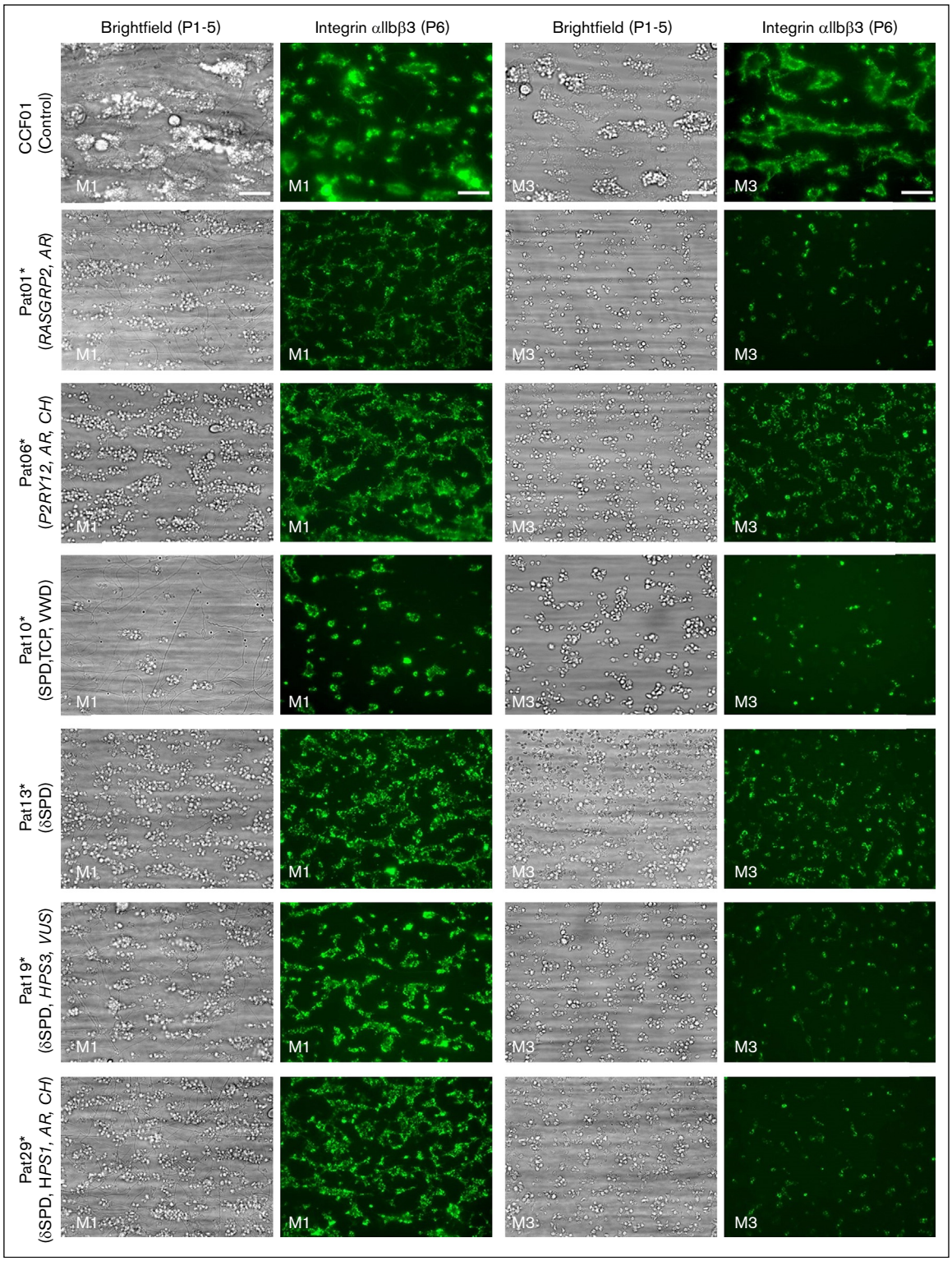

Figure 2. Altered thrombus formation in the blood of index patients with confirmed genetics. Whole blood from patients and control subjects was perfused over microspots from *M1* to *M6* for 3.5 minutes at a wall-shear rate of 1000/s. Brightfield and fluorescence images were captured using an EVOS-FL microscope and a 60× oil objective and analyzed for platelet phenotypes. Shown are representative brightfield and fluorescence (FITC α-fibrinogen mAb for integrin αIIbβ3 activation) images at the end stage (scale bar, 20 μm) for microspots *M1* (collagen 1) and *M3* (collagen 3). Results for a control subject (CCF01), index patients with a defect in *RASGRP2* (Pat01*) or *P2RY12* (Pat06*), SPD with TCP (SPD, VWD, and TCP) (Pat10*), δ-SPD (no variant identified, Pat13*), or compound heterozygous variants of *HPS3* (Pat19*) or *HSP1* (Pat29*) genes. FITC, fluorescein isothiocyanate.

Previously, we assessed the overall extent of platelet aggregation under flow as a measure called thrombus signature, that is, the integrated scaled sum from *P2* to *P6* for all 6 microspots.[14] The ranking of all current subjects based on the thrombus signature showed the highest levels for controls and heterozygous family members, with Pat14* (mild δ-SPD, genetically unexplained) as the exception (Figure 4B). Platelets from this patient showed only a mild decrease in CD63 expression via flow cytometry. Most of the index patients ranked below the CCFs, indicating a low thrombus signature in most cases of bleed diatheses.

To validate this finding, we performed principal component analysis (PCA) including both thrombus and hematologic parameters, using k-means analysis (Figure 5A). PCA revealed that the first cluster consisted of controls, most heterozygous carriers, and Pat14*; a second cluster with the majority of index patients plus 2 carriers; and a third cluster composed of Pats 09, 10, and 11* (SPD with TCP). The corresponding Euclidean distance matrix confirmed the high cohesiveness of the data per cluster (Figure 5B). This approach indicated that the combination of thrombus and hematologic parameters led to clear segregation between index patients (with *RASGRP2*, *P2RY12*, *HPS1*, *HPS3* mutations, or SPD) and unaffected family members and control subjects.

Linkage of thrombus parameters to clinical and laboratory phenotypes

In addition, we evaluated the additive value of routine laboratory measurements by performing another PCA, considering these data as well and using the k-means algorithm. Thus, we compared all data sets of thrombus formation, hematology, and routine platelet phenotyping using LTA and flow cytometry (for values, see supplemental Datafile 1). This resulted in the same clusters as before, with most index patients carrying *RASGRP2*, *P2RY12*, *HSP1*, or *HSP3* variants grouped together (supplemental Figure 6A, color sidebars). As listed in supplemental Figure 7, the variables that mostly contributed (>40%) to the grouping were the parameters of microspots from *M1* to *M3* and *M5*. platelet and red blood cell counts, collagen- and epinephrine-induced platelet aggregation by LTA, and thrombin-induced CD62P and CD63 expression. We concluded that the inclusion of LTA and flow cytometry data resulted in a limited contribution to the separation between affected patients and other subjects. As a negative control analysis, we compared only the hematologic, LTA, and flow cytometry parameters while excluding the microfluidic results. However, this analysis did not discriminate between the index patients and unaffected family members (supplemental Figure 6B).

In the final analysis, we ranked the subjects according to the summed parameters of those from *M1* to *M3* and *M5* and included the data from individual CCFs. The resulting matrix of summed thrombus parameters and blood cell counts was then compared with the key aberrant phenotypic traits per subject (impaired platelet aggregation, flow cytometry, bleeding, and oculoalbinism). Using this information on thrombus formation from the 4 surfaces, it also appeared that almost all of these abnormal phenotypes were grouped together with the microfluidic outcome (Figure 6). Notably, Pats 09, 10, and 11* with SPD and moderate TCP ranked lowest, that is, below the patients with HPS, $P2Y_{12}$, or CalDAG-GEF1 defects, suggesting an additive effect of the low platelet count. In agreement with this whole blood reconstitution experiment, showed a clear dependency of the platelet count (supplemental Figure 8). For all subjects, regression analysis of the platelet count with parameter *M1P1* (platelet adhesion to collagen 1) showed a strong correlation R = 0.62 ($P = .001$), but regression analysis with the corresponding thrombus signature yielded an insignificant R = 0.26 ($P = .14$). This indicated that platelet count was a major factor for platelet adhesion but not for platelet aggregate formation and contraction.

Discussion

In this study with 16 patients with a platelet-based bleeding disorder and 15 asymptomatic relatives, we assessed how the multiparameter measurement of thrombus formation on several coated surfaces can help to identify platelet function defects associated with bleeding. All affected patients were diagnosed before using conventional assays and underwent genetic screening. Cluster analysis of microfluidic outcomes of thrombus formation for all patients and subjects revealed: (1) a consistent contribution of parameters from M1 to M3 and M5 with a common phenotype; (2) an additional contribution of blood cell counts to the cluster separation; (3) a limited additive value of LTA and flow cytometry measurements; and (4) segregation into separate clusters of affected patients and nonaffected relatives and control subjects. Jointly, this brings us to the conclusion that the multiparameter microfluidic method of whole blood platelet function measurement has the potential to aid in the identification of platelet-based bleeding disorders.

In 1 of the patients with increased bleeding (Pat01*, ISTH bleeding score of 7), we identified a novel homozygous splice variant of the *RASGRP2* gene, which encodes a small guanosine triphosphatase regulator, CalDAG-GEFI, causing a lack of protein expression in platelets. This new variant expands the set of 29 previously reported mutations in this gene.[29,30] The protein CalDAG-GEFI is known to be essential for platelet aggregation because of its role in Rap1b-dependent activation of integrin αIIbβ3.[31,32] Indeed, when testing the patient's blood, we observed a severe defect in the flow-dependent aggregates and thrombus formation on all microspots. In contrast, the 3 heterozygous relatives (Pat02-04) with a low bleeding phenotype showed normal thrombus formation profiles.

In Pat05* and Pat06* (family 2) with a bleeding phenotype, we found 2 novel compound heterozygous pathogenic/likely pathogenic variants in the *P2RY12* gene, which were linked to a platelet $P2Y_{12}$ receptor defect. Microfluidic analysis of the patient's blood indicated a clear but incomplete reduction in thrombus formation, likely due to residual platelet activation via $P2Y_1$ receptors. The present compound heterozygosity adds to other described, relatively rare pathogenic variants of the *P2RY12* gene.[12,25,33] In contrast, genotyping of Pat08*, who experienced bleeding after surgery and showed reduced ADP-induced platelet aggregation, revealed 1 heterozygous variant of *P2RY12*. However, in microfluidic testing, thrombus formation was similarly impaired as in the index members of family 2. This suggests a dominant inheritance of the phenotype.

Genotyping of members of family 4 (Pats 09-12) with a platelet storage pool defect and mild TCP (65×10^9/L-94×10^9/L) did not reveal a variant that could explain the phenotype. Thrombus

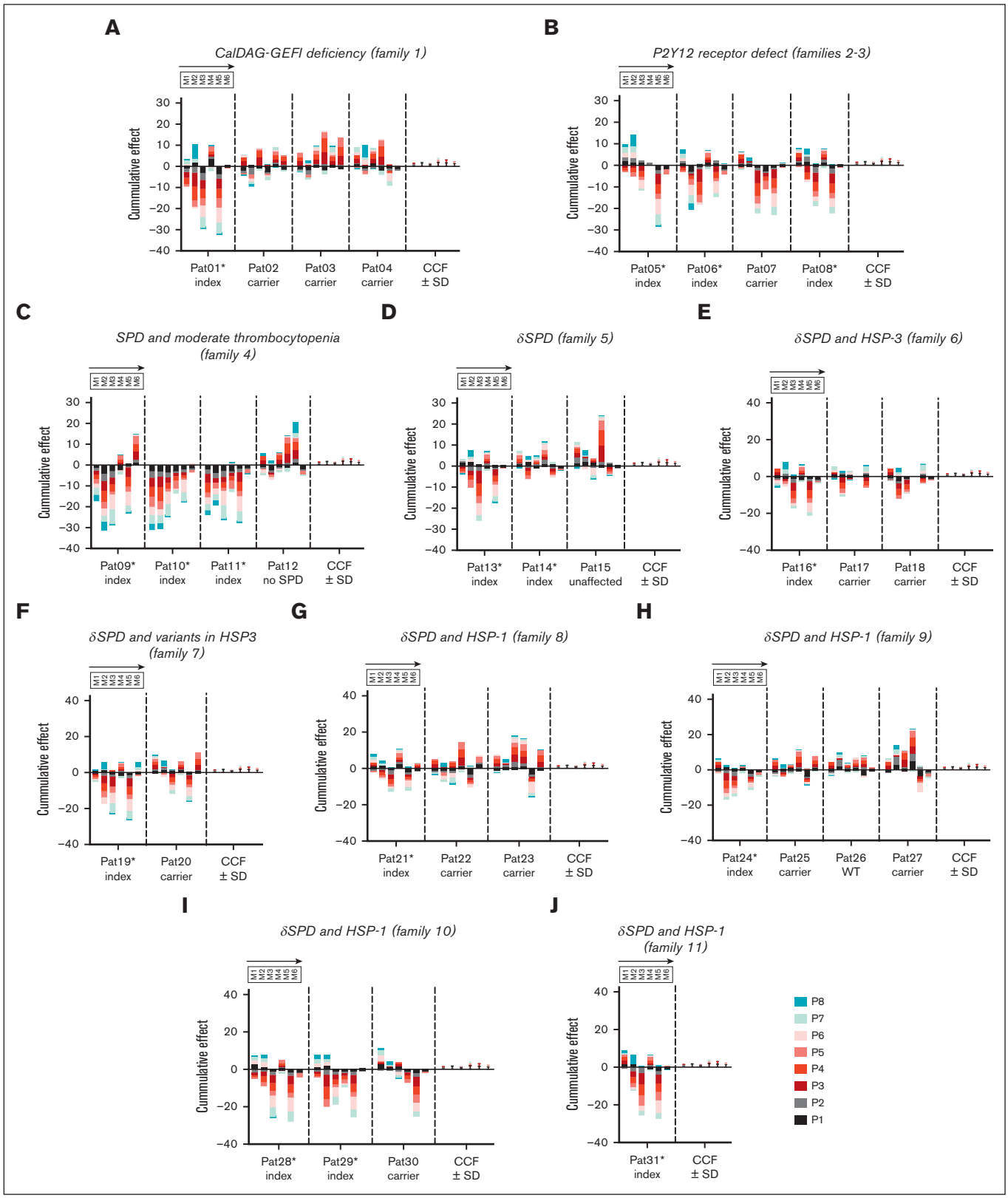

Figure 3. Cumulatively changed parameters of thrombus formation per surface in the included patients. Univariate scaled parameters from *P1* to *P8* of thrombus formation on microspots from *M1* to *M6* were compared per family (I-J) of index (*) and nonindex Pats vs mean values from control subjects (CCF01-05; mean ± standard deviation). Subtracted scaled data were used, as described in supplemental Figure 4. Indicated are cumulative changes in parameters (*P1-8*) vs means of CCF controls (no statistical filtering) per family member; presentation in the order of microspots *M1-6*. For patient description, see Table 1. For raw and scaled data, see supplemental Datafile.

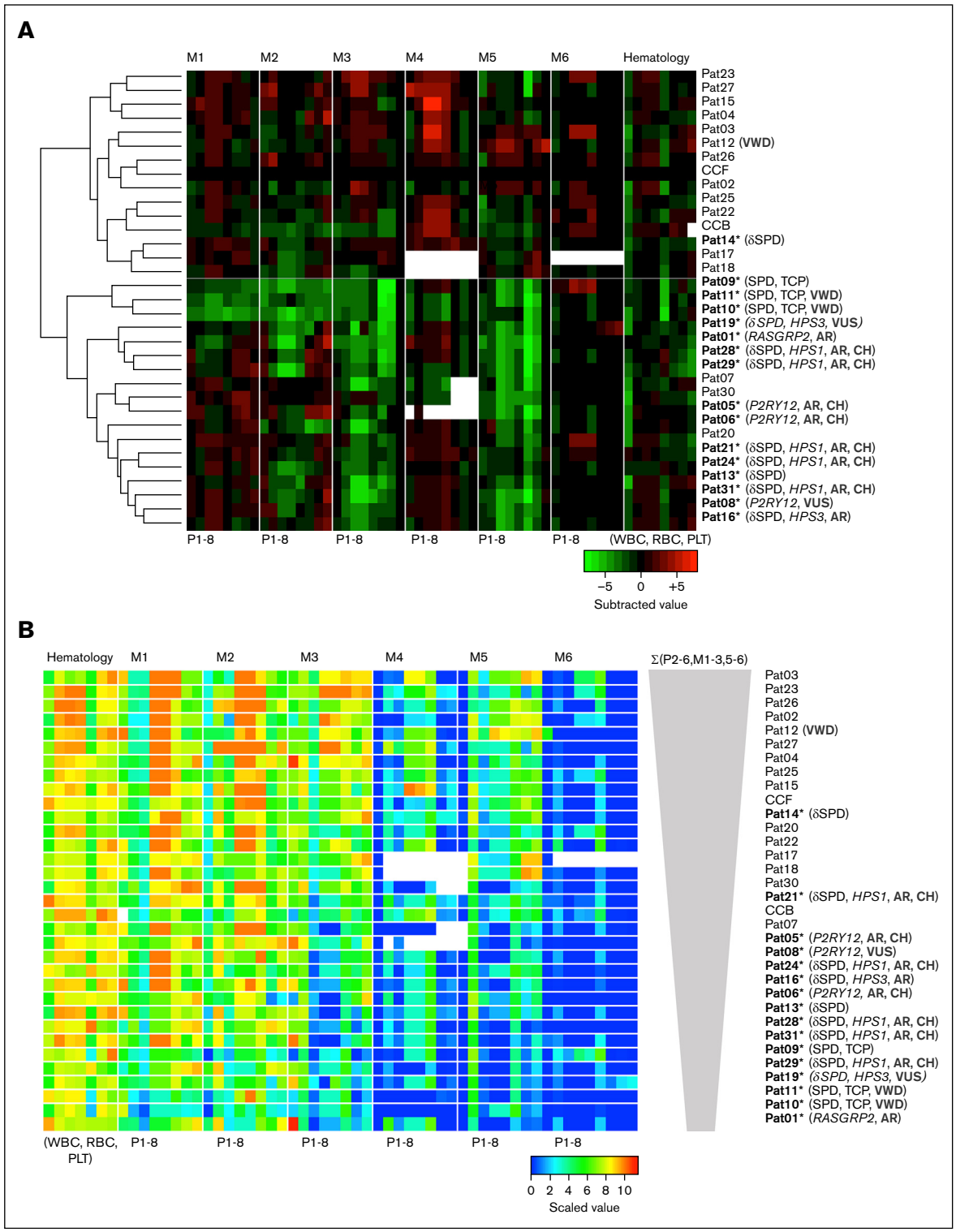

Figure 4. Clustering analysis and signatures of thrombus formation with hematologic parameters. Thrombus formation and hematology data were obtained from 31 patients, family members, and control subjects. (A) Unsupervised clustered heatmap of scaled thrombus parameters (*P1-8*) per microspot (*M1-6*) with added hematologic parameters (WBC, RBC, HGB, HCT, PLT, MPV, RDW, and P-LCR). Shown are subtraction values per patient/family member vs the mean of CCFs. (B) Rearrangement of patient order according to decreasing thrombus signature (Σ*P2-6* for *M1-3* and *M5-6*). Microspot *M4* with missing data was excluded from the thrombus signature analysis. Color coding indicates a decrease (green) or increase (red) in comparison with those of CCFs. AR, autosomal recessive; CH, compound heterozygosity; PLT, platelet; RBC, red blood cell; WBC, white blood cell.

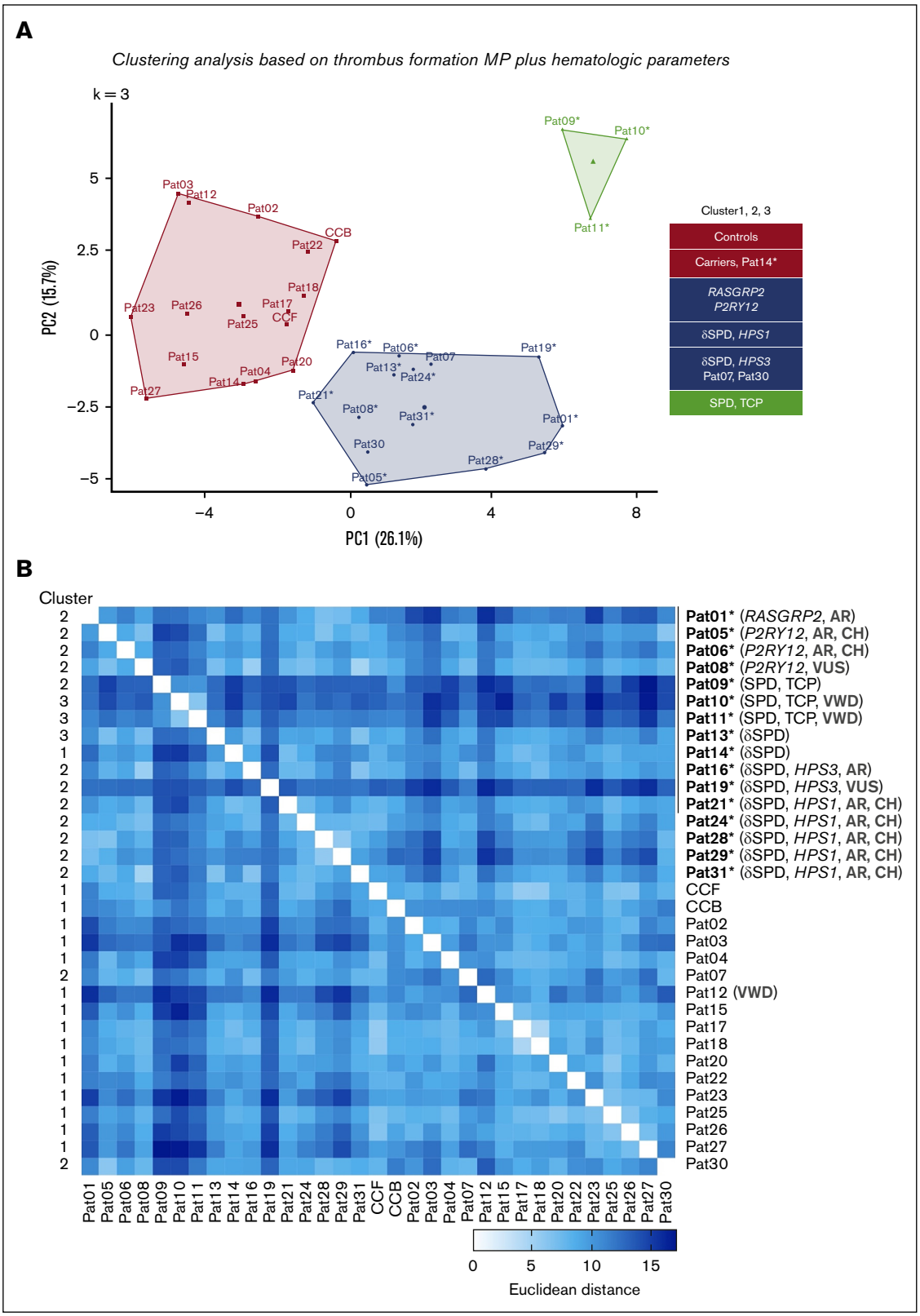

Figure 5. PCA of microspots and hematologic traits of patients and controls. For all included patients, family members, and controls (CCFs and CCBs), multiparameter data (*P1-8*) of thrombus formation on microspots from *M1* to *M6* together with hematologic values, were univariately scaled and clustered for PCA using scaled and mean-centered data (k-means = 3). Missing values were imputed. (A) Default 2-component plot resulting in clusters of (1) controls and most carriers of a heterozygous mutation; (2) most of index patients and autosomal recessive compound heterozygous carriers; (3) family members from Pat 09 to Pat11 with SPD and moderate TCP. (B) Euclidean distance matrix of clustered scaled parameters comparing all individual patients. For values, see supplemental Datafile.

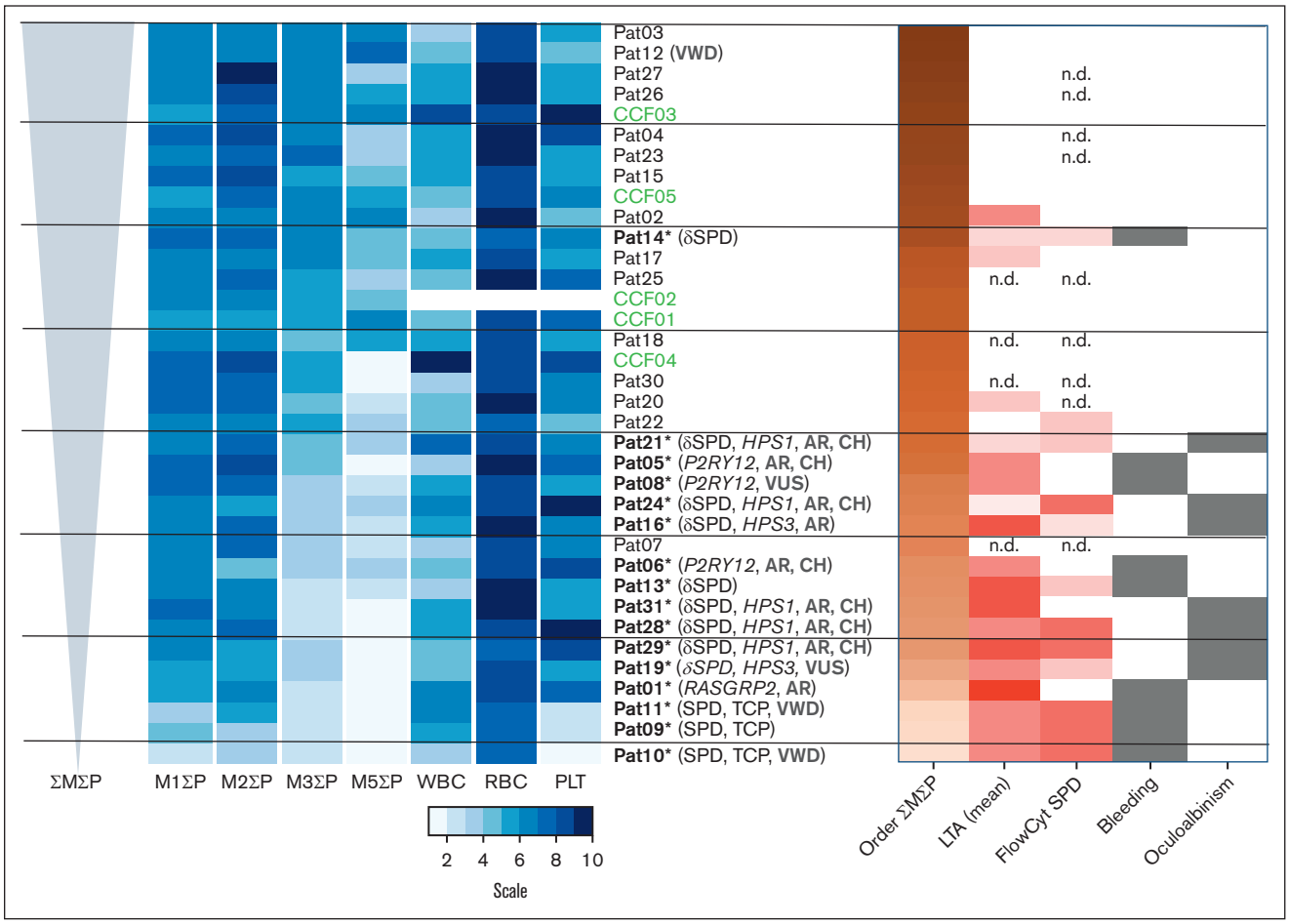

Figure 6. Principal component-based ranking of main microspot parameters separating index patients with bleeding or oculoalbinism. Based on the clustered plots of all compared data sets (supplemental Figure 6A) and the parameters mostly contributing to components 1 or 2 (supplemental Figure 7), the mean parameters of microspots from *M1* to *M3* and *M5* were integrated and ranked, together with hematologic parameters of blood cell counts (WBC, RBC, and PLT). Plotted is the rescaled narrowed data set, ranking individual patients (Pat01-31) and controls (CCF01-05) according to decreasing *ΣMΣP* values. Shown as sidebars are (1) the order of patients (brown color, lowest); (2) mean defects in platelet aggregation (LTA, scaled for ADP, collagen, epinephrine, and ristocetin); (3) mean defects in secretion marker exposure by flow cytometry (FlowCyt) to estimate SPD (thrombin-induced P-selectin and CD63 expression); (4) bleeding phenotype; (5) oculoalbinism phenotype. Color codes: dark red, severely impaired; white, within the control range; gray, reported phenotype. n.d. = not determined.

parameters were very low in Pats 09, 10, and 11*, likely because of TCP. Although the family carried a pathogenic variant in the *VWF* gene, the VWF parameters were within the normal ranges. This family requires further genetic investigation, such as whole exome sequencing or checking for superenhancer sites.[34] Similarly, for family 5 (Pats 13-15), bleeding symptoms and δ-SPD remain genetically unexplained. Pat13*, but not the mother (Pat14*), had overall low parameters of thrombus formation. This is consistent with the lower CD63 expression of platelets from Pat13* compared with that of the mother Pat14*.

The index patients from families 6 to 11 were diagnosed with HPS using flow cytometry and genetic analysis. One exception was Pat19*, whose genetic variants were classified as VUS. Typical symptoms of HPS include oculocutaneous albinism and mild/moderate bleeding diathesis due to a platelet δ–granule secretion defect. Some patients with HPS develop granulomatous colitis and pulmonary fibrosis, depending on the gene affected.[19,35,36] Current knowledge is that HPS is caused by homozygous or compound heterozygous mutations in up to 11 genes including *HPS1* and *HPS3*.[36-38] All index patients of the investigated families carried pathogenic variants in *HPS1* or *HSP3*, whereas the relatives were heterozygous for 1 variant or the wild-type. Interestingly, Pat19* of family 7 displayed compound heterozygous missense variants in *HPS3,* which were classified as VUS. The gene *HPS3* encodes a subunit of the BLOC-2 complex, of which missense variants can lead to milder albinism phenotypes.[37,38] Blood samples from most HPS index patients performed poorly in microfluidic testing and coclustered with samples from patients carrying *RASGRP2* or *P2RY12* mutations.

The integrative analysis of microspot-dependent microfluidic testing in combination with platelet quantitative and qualitative traits had remarkable outcomes. Informative was the ranking of individual subjects based on the cumulative parameters from microspots *M1* to *M3* and *M5*, which separated most of the

patients with a bleeding or albinism phenotype from asymptomatic family members and healthy controls (Figure 6). Following this ranking, thrombus formation was the highest in control subjects and heterozygous carriers. It decreased in the order of *P2RY12* defect (heterozygous or compound heterozygous) > HPS (compound heterozygous *HSP1* or *HSP3*) > *RASGRP2* defect (homozygous) > SPD with TCP.

Microfluidic testing was performed under nonanticoagulant conditions (ie, with a direct thrombin inhibitor), using citrated blood that was recalcified with $CaCl_2$/$MgCl_2$ medium to achieve physiological divalent cation concentrations. This protocol was chosen because it provides optimized platelet adhesion and aggregation under flow, and prevents massive fibrin formation.[16,17] In contrast, the staining of thrombi for exposed phosphatidylserine on platelets in thrombi provides information on the procoagulant activity of a patient's platelets.[17] An extracted heatmap of *P8* from the microspots, however, showed only a clear reduction in this parameter for the Pats 09, 10, and 11* with TCP SPD (supplemental Figure 9), likely because of the limited platelet deposition under flow.

In comparison with earlier studies,[16,39] this study differs in that (1) multiple patients with newly observed mutations were included, (2) clinically and genetically unaffected family members were studied, and (3) a consistent comparison was made between the microfluidic test outcomes and other current diagnostic laboratory tests. The literature provides only incidental flow perfusion studies with a similar number of patients. In a report in which 32 patients with von Willebrand disease were enrolled, microfluidic flow assays were shown to be useful for the detection of VWF defects.[13] Another similarly sized study on patients with gray platelet syndrome focused on genetics and platelet structure.[40] An early large-scale study on SPDs determined only the VWF levels in patient blood samples.[41]

The coclustering of patients with more severe bleeding (*RASGRP2* and *P2RY12* variants) with patients with δ-SPD (*HSP1* or *HSP3* variants) experiencing more moderate bleeding indicated that the reduction in microfluidic thrombus formation revealed impaired hemostasis but not the severity of bleeding. However, a relevant consideration is that 7 of the 16 included index patients are children (age <12 years), in whom bleeding diathesis is more difficult to score.[42]

Taken together, our results indicate that multiparameter microfluidic testing can be of added value for patients with a bleeding disorder as a complementary assay to other diagnostic platelet function tests. However, this study has some limitations. Firstly, in our study, the number of included patients and relatives was still limited, and for confirmative purposes, this number must be increased in the future. Secondly, current and other systems biology approaches need to be used to develop more confined assays in terms of surfaces and parameters while maintaining diagnostic potential. Improvements can also be made by developing fully automated image-analysis scripts. Thirdly, for a standard assay in the diagnostic laboratory, a small and affordable optical device with an easy-to-use flow chip must be developed, providing the same thrombus outcome values for the most discriminative surfaces. Once developed and validated, it is reasonable to state that the device costs are similar to those of other flow-dependent whole blood systems, such as PFA-100 and T-TAS, which measure different aspects of platelet function.[17] Fourthly, further work is required to determine the additive value of controlled coagulation, altered shear rates, and kinetic data in addition to the present conditions.

Acknowledgments

The authors thank Anja Kahle and Eileen Lerner for their excellent technical assistance. I.P. and D.I.F. are supported by the European Union's Horizon 2020 research and innovation program under the Marie Sklodowska-Curie grant agreement TAPAS 766118. D.I.F. was enrolled in a joint PhD program at the Universities of Maastricht and Santiago de Compostela (Spain); I.P. was enrolled in a joint PhD program of the Universities of Maastricht and Reading (United Kingdom). The funders had no role in the study design, data collection and analysis, decision to publish, or preparation of the manuscript.

Authorship

Contribution: B.Z., F.A., and A.K. took care of the patients and their families; D.B., S.F., A.L., and A.D. performed the molecular genetic analysis; M.C. performed western blot analysis and analyzed the data; I.P. and D.I.F. performed the experiments, analyzed the data, and wrote the manuscript; and D.B., B.Z., and J.W.M.H. supervised the study and wrote the manuscript.

Conflict-of-interest disclosure: J.W.M.H. is a consultant at Synapse Research Institute Maastricht. The remaining authors declare no competing financial interests.

ORCID profiles: D.I.F., 0000-0002-5055-9019; M.C., 0000-0002-7880-5250; J.W.M.H., 0000-0002-2848-5121; D.B., 0000-0001-9238-2904; B.Z., 0000-0002-4954-7029.

Correspondence: Johan W. M. Heemskerk, Synapse Research Institute, Koningin Emmaplein 7, 6214 AC Maastricht, The Netherlands; email: jwmheem722@outlook.com; and Barbara Zieger, Department Pediatrics, Medical Center, Mathildenstr. 1, 79106 Freiburg, Germany; email: barbara.zieger@uniklinik-freiburg.de.

References

1. Bastida JM, Benito R, Lozano ML, et al. Molecular diagnosis of inherited coagulation and bleeding disorders. *Semin Thromb Hemost*. 2019;45(7):695-707.
2. Nurden P, Stritt S, Favier R, Nurden AT. Inherited platelet diseases with normal platelet count: phenotypes, genotypes and diagnostic strategy. *Haematologica*. 2021;106(2):337-350.
3. Vries MJ, van der Meijden PE, Kuiper GJ, et al. Preoperative screening for bleeding disorders: a comprehensive laboratory assessment of clinical practice. *Res Pract Thromb Haemost*. 2018;2(4):767-777.

4. Bourguignon A, Tasneem S, Hayward CP. Screening and diagnosis of inherited platelet disorders. *Crit Rev Clin Lab Sci*. 2022;59(6):405-444.
5. Lordkipanidzé M, Lowe GC, Kirkby NS, et al. Characterization of multiple platelet activation pathways in patients with bleeding as a high-throughput screening option: use of 96-well Optimul assay. *Blood*. 2014;123(8):e11-22.
6. Hayward CP, Moffat KA, Brunet J, et al. Update on diagnostic testing for platelet function disorders: what is practical and useful? *Int J Lab Hematol*. 2019;41(suppl 1):26-32.
7. Gresele P, Bury L, Mezzasoma AM, Falcinelli E. Platelet function assays in diagnosis: an update. *Expert Rev Hematol*. 2019;12(1):29-46.
8. Cattaneo M, Cerletti C, Harrison P, et al. Recommendations for the standardization of light transmission aggregometry: a consensus of the working party from the platelet physiology subcommittee of SSC/ISTH. *J Thromb Haemost*. 2013;11(6):1183-1189.
9. Nakamura L, Sandrock-Lang K, Speckmann C, et al. Platelet secretion defect in a patient with stromal interaction molecule 1 deficiency. *Blood*. 2013;122(22):3696-3698.
10. Van Asten I, Schutgens RE, Baaij M, et al. Validation of flow cytometric analysis of platelet function in patients with a suspected platelet function defect. *J Thromb Haemost*. 2018;16(4):689-698.
11. Simeoni I, Stephens JC, Hu F, et al. A high-throughput sequencing test for diagnosing inherited bleeding, thrombotic, and platelet disorders. *Blood*. 2016;127(23):2791-2803.
12. Downes K, Megy K, Duarte D, et al. Diagnostic high-throughput sequencing of 2396 patients with bleeding, thrombotic, and platelet disorders. *Blood*. 2019;134(23):2082-2091.
13. Lehmann M, Ashworth K, Manco-Johnson M, Di Paola J, Neeves KB, Ng CJ. Evaluation of a microfluidic flow assay to screen for von Willebrand disease and low von Willebrand factor levels. *J Thromb Haemost*. 2018;16(1):104-115.
14. Van Geffen JP, Brouns S, Batista J, et al. High-throughput elucidation of thrombus formation reveals sources of platelet function variability. *Haematologica*. 2019;104(6):1256-1267.
15. Nagy M, Mastenbroek TG, Mattheij NJ, et al. Variable impairment of platelet functions in patients with severe, genetically linked immune deficiencies. *Haematologica*. 2018;103(3):540-549.
16. De Witt SM, Swieringa F, Cavill R, et al. Identification of platelet function defects by multi-parameter assessment of thrombus formation. *Nat Commun*. 2014;5:4257.
17. Provenzale I, Brouns SL, van der Meijden PE, Swieringa F, Heemskerk JW. Whole blood based multiparameter assessment of thrombus formation in a standard microfluidic device to proxy in vivo haemostasis and thrombosis. *Micromachines (Basel)*. 2019;10(11):787.
18. Lahav J, Jurk K, Hess O, et al. Sustained integrin ligation involves extracellular free sulfhydryls and enzymatically catalyzed disulfide exchange. *Blood*. 2002;100(7):2472-2478.
19. Boeckelmann D, Wolter M, Neubauer K, et al. Hermansky-Pudlak syndrome: identification of novel variants in the genes HPS3, HPS5, and DTNBP1 (HPS7). *Front Pharmacol*. 2021;12:786937.
20. Richards S, Aziz N, Bale S, et al. Standards and guidelines for the interpretation of sequence variants: a joint consensus recommendation of the American college of medical genetics and genomics and the association for molecular pathology. *Genet Med*. 2015;17(5):405-424.
21. Boeckelmann D, Lenz A, Fels S, Loewecke F, Lausch E, Zieger B. Novel splice-site mutation in RASGRP2 leading to CalDAG-GEFI deficiency. *Blood*. 2020;136(suppl 1):16-17.
22. Dupuis A, Böckelmann D, Laeuffer P, Neubauer K, Gachet C, Zieger B. Two novel compound heterozygous pathogenic variants in P2YR12 gene. *Blood*. 2018;132(suppl 1):1154.
23. Lecchi A, Femia EA, Paoletta S, et al. Inherited dysfunctional platelet $P2Y_{12}$ receptor mutations associated with bleeding disorders. *Haemostaseologie*. 2016;36(4):279-283.
24. Zhang J, Zhang K, Gao ZG, et al. Agonist-bound structure of the human $P2Y_{12}$ receptor. *Nature*. 2014;509(7498):119-122.
25. Daly ME, Dawood BB, Lester WA, et al. Identification and characterization of a novel $P2Y_{12}$ variant in a patient diagnosed with type 1 von Willebrand disease in the European MCMDM-1VWD study. *Blood*. 2009;113(17):4110-4113.
26. Mundell SJ, Rabbolini D, Gabrielli S, et al. Receptor homodimerization plays a critical role in a novel dominant negative $P2RY_{12}$ variant identified in a family with severe bleeding. *J Thromb Haemost*. 2018;16(1):44-53.
27. Sandrock-Lang K, Bartsch I, Buechele N, et al. Novel mutation in two brothers with Hermansky Pudlak syndrome type 3. *Blood Cells Mol Dis*. 2017;67:75-80.
28. Auger JM, Watson SP. Dynamic tyrosine kinase-regulated signaling and actin polymerisation mediate aggregate stability under shear. *Arterioscler Thromb Vasc Biol*. 2008;28(8):1499-1504.
29. Westbury SK, Canault M, Greene D, et al. Expanded repertoire of RASGRP2 variants responsible for platelet dysfunction and severe bleeding. *Blood*. 2017;130(8):1026-1030.
30. Sevivas T, Bastida JM, Paul DS, et al. Identification of two novel mutations in RASGRP2 affecting platelet CalDAG-GEFI expression and function in patients with bleeding diathesis. *Platelets*. 2018;29(2):192-195.
31. Crittenden JR, Bergmeier W, Zhang Y, et al. CalDAG-GEFI integrates signaling for platelet aggregation and thrombus formation. *Nat Med*. 2004;10(9):982-986.

32. Cifuni SM, Wagner DD, Bergmeier W. CalDAG-GEFI and protein kinase C represent alternative pathways leading to activation of integrin αIIbβ3 in platelets. *Blood*. 2008;112(5):1696-1703.

33. Lecchi A, Razzari C, Paoletta S, et al. Identification of a new dysfunctional platelet $P2Y_{12}$ receptor variant associated with bleeding diathesis. *Blood*. 2015;125(6):1006-1013.

34. Petersen R, Lambourne JJ, Javierre BM, et al. Platelet function is modified by common sequence variation in megakaryocyte super enhancer. *Nat Commun*. 2017;8:16058.

35. Oh J, Ho L, Ala-Mello S, et al. Mutation analysis of patients with Hermansky-Pudlak syndrome: a frameshift hot spot in the HPS gene and apparent locus heterogeneity. *Am J Hum Genet*. 1998;62(3):593-598.

36. Pennamen P, Le L, Tingaud-Sequeira A, et al. BLOC1S5 pathogenic variants cause a new type of Hermansky-Pudlak syndrome. *Genet Med*. 2020; 22(10):1613-1622.

37. Huizing M, Malicdan MC, Wang JA, et al. Hermansky-Pudlak syndrome: mutation update. *Hum Mutat*. 2020;41(3):543-580.

38. Boeckelmann D, Wolter M, Käsmann-Kellner B, Koehler U, Schieber-Nakamura L, Zieger B. A novel likely pathogenic variant in the BLOC1S5 gene associated with Hermansky-Pudlak syndrome type 11 and an overview of human BLOC-1 deficiencies. *Cells*. 2021;10:2630.

39. Nagy M, van Geffen JP, Stegner D, et al. Comparative analysis of microfluidics thrombus formation in multiple genetically modified mice: link to thrombosis and hemostasis. *Front Cardiovasc Med*. 2019;6:99.

40. Sims MC, Mayer L, Collins JH, et al. Novel manifestations of immune dysregulation and granule defects in gray platelet syndrome. *Blood*. 2020;136(17): 1956-1967.

41. Witkop CJ, Bowie EJ, Krumwiede MD, Swanson JL, Plumhoff EA, White JG. Synergistic effect of storage pool deficient platelets and low plasma von Willebrand factor on the severity of the hemorrhagic diathesis in Hermansky-Pudlak syndrome. *Am J Hematol*. 1993;44(4):256-259.

42. Achey MA, Nag UP, Robinson VL, et al. The developing balance of thrombosis and hemorrhage in pediatric surgery: clinical implications of age-related changes in hemostasis. *Clin Appl Thromb Hemost*. 2020;26:1076029620929092.